Physiologically Based Pharmacokinetic Modeling Approaches for Patients With SARS-CoV-2 Infection: A Case Study With Imatinib

Jeffry Adiwidjaja, PhD[1,2] iD **, Josephine A. Adattini, PhD[1]** iD **, Alan V. Boddy, PhD[3]** iD **, and Andrew J. McLachlan, PhD[1]** iD

Abstract

Severe acute respiratory syndrome coronavirus 2 (SARS-CoV-2) infection, which causes coronavirus disease 2019 (COVID-19), manifests as mild respiratory symptoms to severe respiratory failure and is associated with inflammation and other physiological changes. Of note, substantial increases in plasma concentrations of α_1-acid-glycoprotein and interleukin-6 have been observed among patients admitted to the hospital with advanced SARS-CoV-2 infection. A physiologically based pharmacokinetic (PBPK) approach is a useful tool to evaluate and predict disease-related changes on drug pharmacokinetics. A PBPK model of imatinib has previously been developed and verified in healthy people and patients with cancer. In this study, the PBPK model of imatinib was successfully extrapolated to patients with SARS-CoV-2 infection by accounting for disease-related changes in plasma α_1-acid-glycoprotein concentrations and the potential drug interaction between imatinib and dexamethasone. The model demonstrated a good predictive performance in describing total and unbound imatinib concentrations in patients with SARS-CoV-2 infection. PBPK simulations highlight that an equivalent dose of imatinib may lead to substantially higher total drug concentrations in patients with SARS-CoV-2 infection compared to that in patients with cancer, while the unbound concentrations remain comparable between the 2 patient populations. This supports the notion that unbound trough concentration is a better exposure metric for dose adjustment of imatinib in patients with SARS-CoV-2 infection, compared to the corresponding total drug concentration. Potential strategies for refinement and generalization of the PBPK modeling approach in the patient population with SARS-CoV-2 are also provided in this article, which could be used to guide study design and inform dose adjustment in the future.

Patients with severe acute respiratory syndrome coronavirus 2 (SARS-CoV-2) infection often present with dyspnea and pneumonitis, which may progress to an acute respiratory distress syndrome.[1] In addition to the pulmonary manifestations, acute renal impairment has been recognized as a prevalent complication of the disease.[2–4] Patients with SARS-CoV-2 infection and preexisting chronic hepatic impairment, particularly severe liver cirrhosis, tended to have a poor prognosis.[5] SARS-CoV-2 infection has also been associated with acute liver injury (characterized by a substantial increase in alanine aminotransferase),[5] with moderate and severe liver injury present in 21% and 6% of patients, respectively, who tested positive for SARS-CoV-2 infection in a large US cohort.[6] Total plasma concentrations of imatinib, a kinase inhibitor that binds extensively to plasma α_1-acid-glycoprotein (AAG), were considerably higher in patients with severe SARS-CoV-2 infection than those reported in patients with cancer.[7] Understanding (patho)physiological changes in patients with SARS-CoV-2 infection is of clinical importance to help guide optimal dosing regimens of drugs for individual patients.

Physiologically based pharmacokinetic (PBPK) modeling approaches may provide valuable mechanistic insights into disease-related changes in drug pharmacokinetics in patients with SARS-CoV-2. PBPK modeling and simulation is also best positioned

[1]Sydney Pharmacy School, Faculty of Medicine and Health, The University of Sydney, Sydney, New South Wales, Australia
[2]Division of Pharmacotherapy and Experimental Therapeutics, UNC Eshelman School of Pharmacy, University of North Carolina at Chapel Hill, Chapel Hill, North Carolina, USA
[3]UniSA Cancer Research Institute and UniSA Clinical & Health Sciences, University of South Australia, Adelaide, South Australia, Australia

Corresponding Author:
Andrew J. McLachlan, PhD, Sydney Pharmacy School, Faculty of Medicine and Health, The University of Sydney, Sydney, NSW 2006, Australia
Email: andrew.mclachlan@sydney.edu.au

to identify and predict the extent of drug interactions in this patient population and to predict interpatient variability in drug pharmacokinetics due to the complex interplay between SARS-CoV-2 infection and comorbidities. A virtual population of patients with SARS-CoV-2 infection that accounts for key clinical features of the disease pertinent to drug disposition is pivotal for reliable PBPK model–based predictions. This study aimed to extend the use of a PBPK modeling approach to predict drug pharmacokinetics in patients with SARS-CoV-2 infection, using imatinib as an illustrative example.

Methods

All population-based PBPK modeling and simulations were performed using the Simcyp Simulator (version 20 release 1, Certara UK Limited, Simcyp Division, Sheffield, UK) with the default "general North European Caucasian" as the base virtual population. The mean plasma concentrations of AAG were modified from the Simcyp default value in healthy adult males of 0.79 g/L (coefficient of variation [CV] 23%) to 0.90 g/L (CV 30%) for the gastrointestinal stromal tumor (GIST) cohort[8] and 1.93 g/L (CV 30%) for the SARS-CoV-2 patient cohort.[7] The default female-to-male ratio in AAG concentrations of 0.9 was maintained throughout the simulations. An accurate representation of plasma AAG concentrations is critical for PBPK model predictions of imatinib concentrations due to its extensive binding to this protein.[9,10]

Drug-related input parameters and key assumptions underpinning the PBPK model of imatinib have been detailed previously, as summarized in Table S1.[11] As a basic compound, imatinib binds extensively to AAG.[9] The unbound fraction in plasma (fu_p) of 0.05 for AAG binding was assigned to the PBPK model of imatinib based on the reported value in healthy European populations.[12,13] The corresponding dissociation constant was fixed and assumed to be independent of plasma AAG concentrations. Therefore, the variability in fu_p reflected interindividual variability and disease-related changes in AAG concentrations. The intrinsic clearances of imatinib to N-desmethyl imatinib and other metabolites were estimated from in vitro kinetic data using recombinant cytochrome P450 (CYP) 3A4 and human liver microsomes (in the presence of azamulin) as detailed in Table S1. The latter represented the CYP2C8 metabolism pathway, assuming very minor contribution (≈3%) of the other CYP enzymes to imatinib metabolism.[14] The mechanism based inhibition (MBI) of CYP3A4 following chronic administration of imatinib was modeled by an increase in degrada-

tion of the active enzyme and, thus, a decrease in enzyme activity over time, based on a turnover model as detailed elsewhere.[15] PBPK model predictions that incorporated a CYP3A4 MBI of imatinib were consistent with the clinically observed interactions with a range of CYP3A modulators; however, apparent clearance of imatinib was underestimated. Hence, a non–pathway-specific additional clearance (additional intrinsic clearance) was assigned to the PBPK model of imatinib at steady state to correct this underprediction. The PBPK model of imatinib has been verified extensively using clinical pharmacokinetic data from healthy and disease populations (GIST and chronic myeloid leukemia [CML]).[11,16] The PBPK model was reverified using clinically observed total and unbound imatinib concentrations in patients with GIST,[8] given that the model was developed using a previous version of the Simcyp Simulator (version 17).

Previously published clinical pharmacokinetic data of imatinib in patients with reverse transcription polymerase chain reaction test-confirmed SARS-CoV-2 infection[7,17] was retrieved from the original publication using the WebPlotDigitizer version 4.2 (www.automeris.io/WebPlotDigitizer). Reported unbound imatinib concentration in the patient population with SARS-CoV-2 that were below half of the lowest limit of quantitation (50 μg/L)[7] were excluded (2 sampling points). Since most of the patients in this cohort (≈70%) also received dexamethasone,[17] PBPK simulations were performed with and without coadministration of dexamethasone (6 mg daily orally). Dexamethasone 6 mg/day intravenously or orally for up to 10 days or until hospital discharge is recommended for treatment of hospitalized adults with severe SARS-CoV-2 infection who require supplemental oxygen or mechanical ventilation.[18] PBPK input parameters for dexamethasone are summarized in Table S1. The PBPK model of dexamethasone was verified using clinical pharmacokinetic data in patients with community-acquired pneumonia and in the patient population with SARS-CoV-2 (Table 1), the latter of which implemented a sparse sampling strategy. The patient cohort with SARS-CoV-2 also received remdesivir (200 mg loading dose on day 1, followed by 100 mg daily given as a short-term intravenous infusion) as part of the treatment regimen. Hence, the potential CYP3A inhibitory effect by remdesivir on dexamethasone metabolism (dexamethasone may act as both a substrate and inducer of CYP3A enzymes) was accounted for in the simulation. A previously published PBPK model of remdesivir[19] was employed with additional parameter of CYP3A inhibitory constant (K_i) of 0.8 μmol/L,[20] assuming a competitive inhibition of the isoenzymes.

Table 1. Summary of Clinical Studies Used to Verify the PBPK Models of Imatinib and Dexamethasone and Comparison Between Clinically Reported Values and PBPK Model Predictions of Key Pharmacokinetics Parameters of the Drugs

Drug	Patient Characteristics	Pharmacokinetic Parameter	Clinically Reported Value	PBPK Model Prediction	PBPK Model Prediction (With Modulator)[a]	Prediction Fold Difference[b] Monotherapy	With Modulator
Imatinib[7,17]	Patients being hospitalized with SARS-CoV-2 infection (n = 134, 30 women), with median age of 64 years (IQR, 57-73) and plasma AAG level of 1.93 g/L (IQR, 1.64-2.28), receiving imatinib (400 mg daily with an 800-mg loading dose). Comedications included dexamethasone (88 patients), remdesivir (30 patients), chloroquine (14 patients), and PPI (49 patients). Plasma samples were collected up to 9 days after commencement of treatment. Unbound plasma concentrations of imatinib were measured in plasma samples from 38 patients receiving at least 3 doses of imatinib.	$C_{ss,max}$ (µg/L)[c]	7157 (IQR, 4358-11 761)[d]	4668	4374	0.65	0.61
			5983 (IQR, 2504-8346)[d]			0.78	0.73
		$C_{ss,min}$ (µg/L)[c]	2156 (IQR, 738-4179)[d]	2266	2036	1.05	0.94
			1791 (IQR, 928-3204)[d]			1.27	1.14
		$C_{ss,max,u}$ (µg/L)	80.7 (IQR, 44.7-158.6)[d]	102.1	101.7	1.27	1.26
		$C_{ss,min,u}$ (µg/L)	38.0 (IQR, 31.5-56.9)[d]	49.4	49.2	1.30	1.29
Dexamethasone[21]	Patients with community-acquired pneumonia (n = 15, 2 women), aged 68.5 ± 13.3 years, with a median BMI of 27.5 kg/m² (IQR, 25.2-30.4), being treated with dexamethasone (6 mg per oral daily). Plasma samples were taken at day 1 of treatment.	$AUC_{0-\infty}$ (µg·h/L) CL/F (L/h)	774 (IQR, 146)[d] 7.7 (IQR, 5.2-9.7)[d]	651.1 9.2	NA N.A.	0.84 1.19	NA NA
Dexamethasone[22]	2 male patients admitted to hospital with SARS-CoV-2 infection (41 and 52 years of age), receiving both dexamethasone (6 mg) and remdesivir (100 mg) as part of the treatment regimen. Plasma samples were collected for up to 6 days.[e]	$C_{max,ss}$ (µg/L) C_{20h} (µg/L)	64.17- 76.58 2.73-8.34	70.73 16.46	71.21 16.59		

AAG, α_1-acid-glycoprotein; $AUC_{0-\infty}$, area under the plasma concentration–time curve from time 0 to infinity; C_{20h}, plasma concentration at 20 hours after dosing; CL/F, apparent clearance; $C_{max,ss}$, peak plasma concentration at steady state; $C_{max,ss,u}$, unbound peak plasma concentration at steady state; $C_{min,ss}$, trough plasma concentration at steady state; $C_{min,ss,u}$, unbound trough plasma concentration at steady state; IQR, interquartile range; NA, not applicable; PPI, proton pump inhibitor.

[a] PBPK model predicted values in the presence of coadministration with either dexamethasone (for imatinib) or remdesivir (for dexamethasone).

[b] Prediction fold differences expressed as the ratio of PBPK prediction to clinically observed values.

[c] Two different clinically reported values each correspond to the subsets of patient cohort used for development and verification of the population pharmacokinetic model of imatinib, respectively.[7]

[d] Reported as median values with the corresponding IQR.

[e] For comparison with the PBPK simulations, all the samples were assumed to be collected at day 4 after initiation of treatment.

PBPK simulations of imatinib and dexamethasone pharmacokinetics were performed with trial designs (number of patients, age range, proportion of male/female patients, and dosing regimens) matched to the corresponding clinical studies (Table 1). A total of 10 virtual trials for each simulation were carried out. Clinically observed concentrations of imatinib and dexamethasone were superimposed to simulated
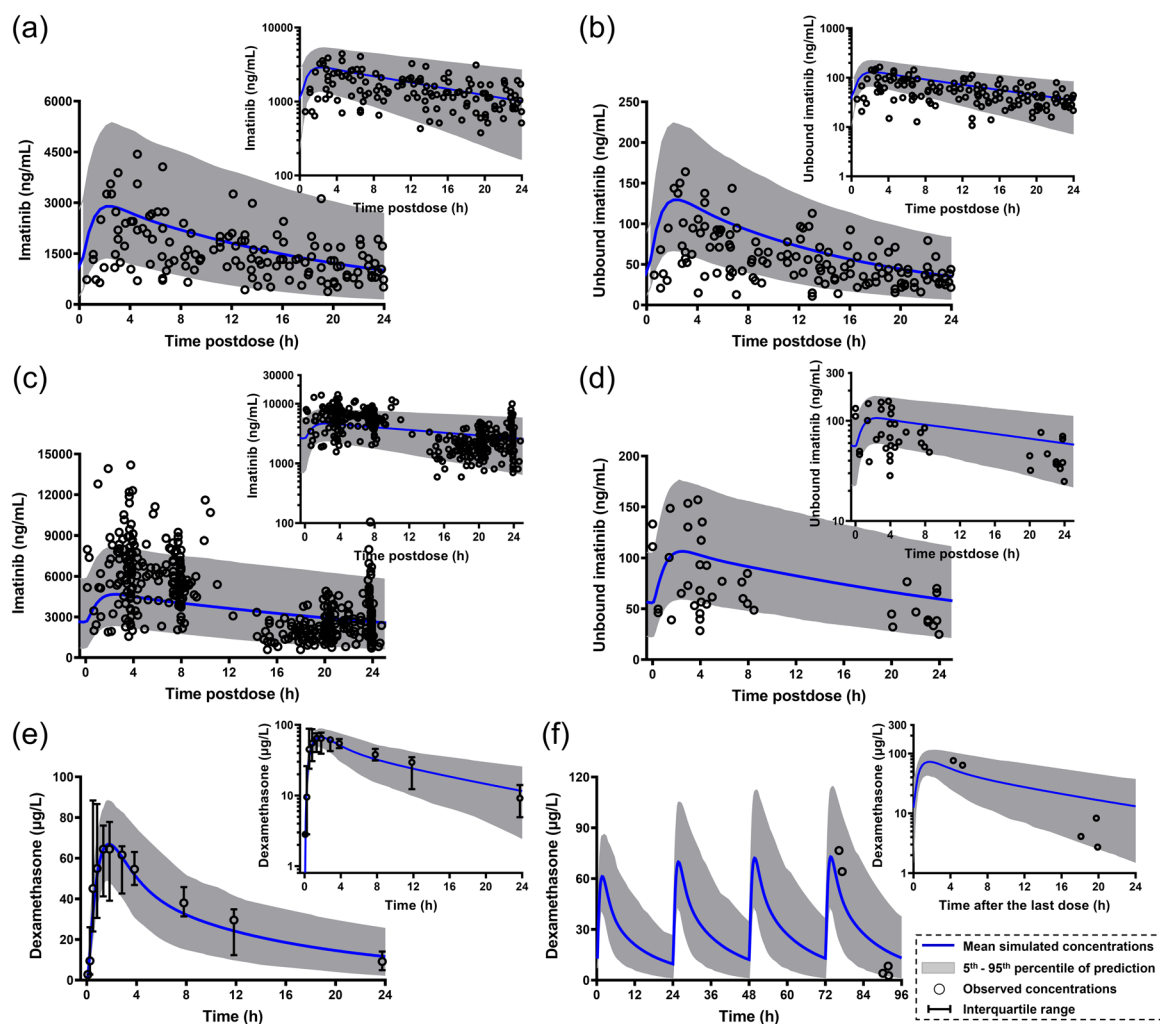
Figure 1. Physiologically based pharmacokinetic (PBPK) model predictions of total and unbound plasma concentrations of imatinib in patients with gastrointestinal stromal tumor (a, b) and in a patient cohort with severe acute respiratory syndrome coronavirus 2 (SARS-CoV-2) (c, d). Comparison of PBPK simulations and clinically observed concentrations of dexamethasone (6 mg) given as a single oral dose in patients with community-acquired pneumonia (e) and as multiple oral doses in patients with SARS-CoV-2 infection (f). Mean simulated concentrations (blue lines) and the prediction interval (5th to 95th percentile as gray area) are depicted in linear scale with the corresponding semilogarithmic plots as insets. Clinically observed individual (a-d, f) and median plasma concentrations (e) are represented by the black circles.

profiles for a visual inspection of predictive performance. Prism version 9.3.0 (GraphPad Software, San Diego, California) was used to generate the simulated plots. The ratios of predicted to observed pharmacokinetic parameters of the drugs were also calculated.

Results

Clinically observed concentrations of imatinib in patients with GIST were well predicted by the PBPK model. More than 90% of the total and 85% of the unbound (free) drug concentrations fell within the prediction interval (5th to 95th percentile of PBPK model predictions), as shown in Figure 1A and B. Similarly, PBPK simulations were able to describe pharmacokinetic profiles of imatinib in patients with SARS-

CoV-2 infection, evaluated by a visual inspection of the simulated pharmacokinetic profiles of both total and free (unbound) imatinib (Figure 1C and D, respectively). However, total peak concentrations of imatinib at steady state ($C_{ss,max}$) appeared to be underestimated with prediction fold differences (ratios of predicted to observed pharmacokinetic parameters) of 0.6 to 0.8 (Table 1).

Incorporation of CYP3A induction by concomitantly administered dexamethasone in the PBPK simulation slightly improved the prediction fold difference of trough concentrations of imatinib ($C_{ss,min}$), but not $C_{ss,max}$ (Table 1), where the prediction fold differences for imatinib $C_{ss,min}$ were reduced from 1.05 to 0.94 and from 1.27 to 1.14 for the first and second subset of the clinical data set, respectively.[7] Verification of
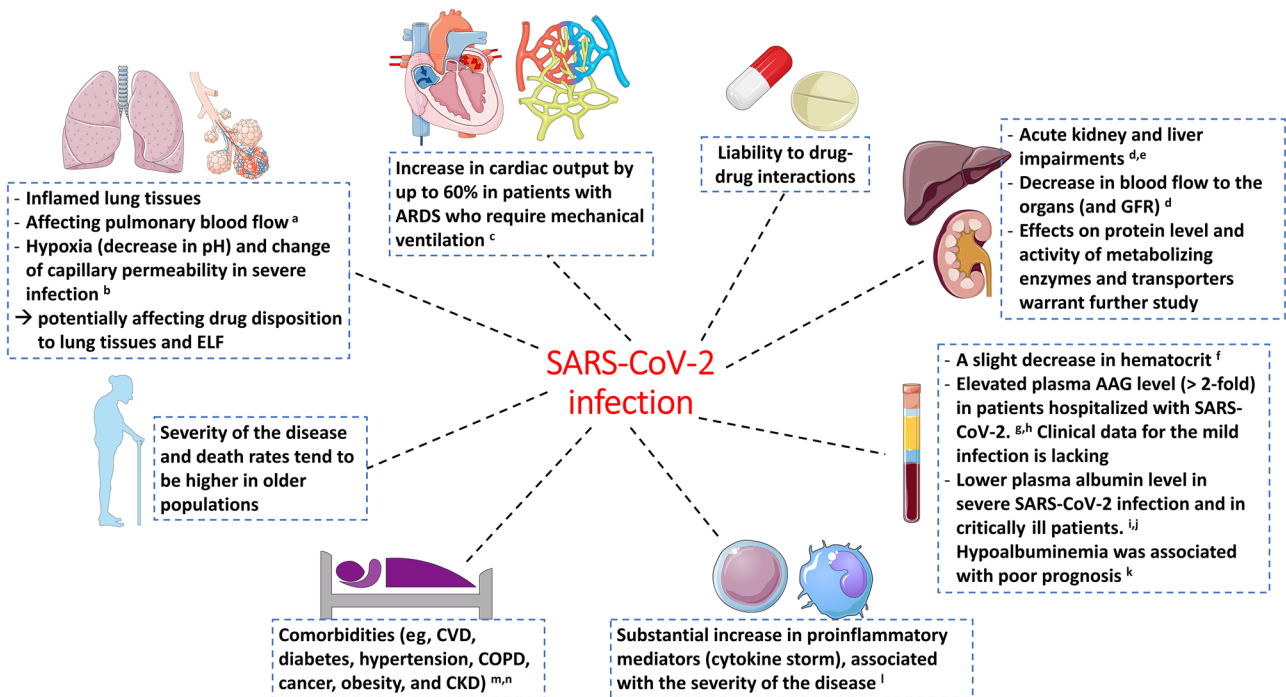
Figure 2. Summary of physiological changes and interacting factors that may explain interindividual variability in pharmacokinetics and response to drugs in patients with SARS-CoV-2 infection. All the illustrations were taken from the Servier Medical Art (SMART, https://smart.servier.com). a,[71] b,[72] c,[73] d,[2] e,[45] f,[74] g,[7] h,[43] i,[60] j,[61] k,[75] l,[36] m,[76] n.[77] AAG, α_1-acid-glycoprotein; ARDS, acute respiratory distress syndrome; CVD, cardiovascular disease; CKD, chronic kidney disease; COPD, chronic obstructive pulmonary disease; ELF, epithelial lining fluid; GFR, glomerular filtration rate; SARS-CoV-2, severe acute respiratory syndrome coronavirus 2.

the PBPK model was limited by a paucity of clinical pharmacokinetic data for dexamethasone in patients with SARS-CoV-2. The model was first verified using clinically observed plasma concentrations from patients with community-acquired pneumonia[21] given some similarities in clinical features and respiratory-related symptoms (eg, dyspnea and lung inflammations) compared to those of SARS-CoV-2 infection. The PBPK model of dexamethasone was also verified using sparsely sampled plasma concentrations from a patient cohort with SARS-CoV-2,[22] with a reasonable predictive performance (Figure 1F).

Physiological changes observed in patients with SARS-CoV-2 infection that are relevant for further improvement and generalization of the PBPK modeling approach in this patient population are outlined in Figure 2. It is noteworthy that this was by no means an exhaustive summary of clinical information collated from the literature.

Discussion

The current study successfully implements a PBPK modeling approach to simulate total and unbound concentrations of imatinib in patients with SARS-CoV-2 infection. This finding supports the use of a PBPK modeling approach for prediction of pharmacokinetics

of new and repurposed drugs for potential treatment of SARS-CoV-2 infection and may help inform or predict previously unstudied drug interactions in this patient population.

There was good agreement between the PBPK model prediction and clinically observed concentrations of imatinib at steady state in patients with GIST (Figure 1A and B). This illustrates the capability of a PBPK modeling approach to predict interpatient variability in imatinib pharmacokinetics by accounting for the variability in plasma AAG concentration and other physiological characteristics underlying pharmacokinetic variability (eg, protein level of CYP3A4 and CYP2C8, which together account for the majority of imatinib metabolism).[9] Population distributions of AAG concentrations reflect the variability in fu_p and contribute to interindividual variability in total hepatic clearance, as accounted for in the PBPK simulations. Similarly, considering the substantial increase in plasma AAG concentrations observed in patients with SARS-CoV-2 infection (up to 2.4-fold increase compared to that in healthy individuals and patients with CML or GIST) is predictive of disease-related changes in imatinib pharmacokinetics in this patient population.

PBPK model predictions of both total and unbound concentrations of imatinib were in concordance with

the corresponding clinical pharmacokinetic data in patients with SARS-CoV-2 (Figure 1C and D), despite slight underpredictions of imatinib $C_{ss,max}$. This disparity was likely due to the disease-related alteration in drug distribution, which was not accounted for in the current PBPK model. Indeed, a population pharmacokinetic analysis hinted at a 60% lower apparent volume of distribution of imatinib in a SARS-CoV-2 population compared to that of patients with CML/GIST.[7] The currently available in silico methods within the PBPK platforms for prediction of tissue-to-plasma partition coefficients lack the capability to account for disease-associated changes of fu_p on the estimated tissue-to-plasma partition coefficient values.[23] This emphasizes the necessity to refine the in silico prediction methods using a more mechanistic approach. This is also the case for transporter-mediated alteration in apparent volume of distribution due to drug interactions or disease-related changes in abundance of drug transporters, which the current PBPK platforms cannot predict.[24] Despite a trend for underprediction of imatinib $C_{ss,max}$ in patients with SARS-CoV-2 infection, the model has a potential to predict responses to imatinib (efficacy and treatment-related adverse effects), which are likely driven by the unbound drug concentrations, as seen with GIST and CML.[25–27]

Systemic exposures to imatinib following a multiple-dosing regimen were significantly affected by coadministration of carbamazepine (a relatively potent CYP3A inducer),[28] but not ritonavir (a strong CYP3A inhibitor).[29] This suggests that at steady state, imatinib is more susceptible to induction compared to inhibition of CYP3A enzymes. Meanwhile, dexamethasone has been reported as a substrate and dose-dependent inducer of CYP3A, with evidence for interactions with probe drugs of the isoenzymes.[30] Hence, the potential drug interaction between imatinib and dexamethasone was accounted for in the PBPK simulations. Despite only slight improvement of the model predictions (Table 1), it is important to account for drug interactions with dexamethasone to increase the mechanistic interpretability and representation of the PBPK model in patients with SARS-CoV-2 infection, particularly to predict complex drug interaction scenarios (eg, multiple comedications with CYP3A substrates and/or modulators). Importantly, as the extent of in vivo CYP3A induction by dexamethasone varies greatly between CYP3A substrates (victim drugs) and dosing regimens of dexamethasone,[30] the current case study with imatinib may help streamline future endeavors to refine the PBPK modeling approaches in patients with SARS-CoV-2 infection.

It is worth mentioning that dexamethasone has been reported to increase the accumulation of substrates of breast cancer resistance protein (BCRP) in cell lines overexpressing BCRP, either through direct inhibition or downregulation of the transporter.[31,32] However, coadministration of dexamethasone is unlikely to affect imatinib absorption. Imatinib is almost completely bioavailable[33] despite being a substrate of both (P-glycoprotein [P-gp] or multidrug resistance protein 1) and BCRP transporters and highly ionized at gastrointestinal pH.[9] This highlights the importance of uptake transporter(s) in the enterocytes that outweighs the intestinal efflux of imatinib mediated by P-gp and BCRP. However, available clinical evidence has been conflicting as to which transporter is primarily responsible for the uptake of imatinib, as has been summarized previously.[16] Hence, the potential effect of intestinal BCRP suppression by concomitant oral administration of dexamethasone on imatinib pharmacokinetics in patients with SARS-CoV-2 infection is unlikely to be of clinical importance.

Potential clinical relevance of CYP3A inhibition by remdesivir on dexamethasone pharmacokinetics has also been explored, since the patient cohort received both drugs. Dexamethasone is a substrate and inducer of CYP3A4, with fraction metabolized of ≈ 0.9.[34,35] Remdesivir was predicted to have little to no impact on dexamethasone clearance due to a relatively short half-life (≈ 1 hour) following a 30-minute intravenous infusion. Meanwhile, the longer-circulating metabolites of remdesivir (GS-704277 and GS-441524) have not been identified as CYP3A inhibitors. Nevertheless, peak concentrations of the metabolites were lower by 1 order of magnitude compared to the parent drug.[19] Further verification of the PBPK model of dexamethasone using larger clinical pharmacokinetic data in patients with SARS-CoV-2 is warranted as the data become available (eg, the ongoing clinical trial NCT04996784; https://clinicaltrials.gov).

Serum levels of interleukin-6 (IL-6), a proinflammatory cytokine able to suppress CYP3A activity, were markedly elevated in severe and nonsevere (mild) SARS-CoV-2 infections with typical mean values of 56.8 (range, 41.4-72.3) and 17.3 (range, 13.5-21.1) pg/mL, respectively,[36] compared to an average value of 5.2 pg/mL in healthy populations.[37] Serum IL-6 concentration of at least 80 pg/mL has also been proposed as a predictive cutoff for respiratory failure (acute respiratory distress syndrome) and the need for mechanical ventilation.[38] However, CYP3A suppression by IL-6 is unlikely to influence systemic exposures of imatinib. Imatinib inhibits its own CYP3A4-mediated metabolism through an MBI,[14] rendering limited residual CYP3A4 activity, which can further be inhibited (suppressed) by IL-6. Interestingly, the CYP3A-mediated hydroxylation of midazolam in patients with moderate to severe SARS-CoV-2 infections was reduced only to a minor extent (22%) compared to

the baseline value (after recovery from the infection).[39] However, the potential effect of elevated serum IL-6 level on the pharmacokinetics of other CYP3A substrates and on the activity of other CYP enzymes (ie, CYP1A2 and CYP2C19) in SARS-CoV-2 infection should be considered.[39] It is worth mentioning that dexamethasone as an anti-inflammatory corticosteroid drug may downregulate the production of IL-6, potentially offsetting its CYP suppression activity. A complex semimechanistic turnover model may provide further insights into the dynamic interplay between IL-6 and dexamethasone on net CYP3A activity. Coadministration of tocilizumab, a monoclonal antibody against the IL-6 receptor, may further attenuate the CYP3A suppression by IL-6. Tocilizumab as a single intravenous dose, in combination with dexamethasone, may be recommended for treatment of severe SARS-CoV-2 infection.[40] Meanwhile, monoclonal antibodies targeting the spike protein of SARS-CoV-2 (eg, sotrovimab), which are recommended to treat patients with mild to moderate SARS-CoV-2 infection who are at high risk of clinical progression,[41] have not been identified to affect in vivo activity of CYP enzymes.

Sensitivity analyses were performed to identify potentially influential parameters in the PBPK model of imatinib to reasonably capture the clinically observed concentrations in patients with SARS-CoV-2 infection, as outlined in Figure S1. Of all the explored parameters, plasma AAG concentration was the most important determinant for total imatinib concentrations in the patient population with SARS-CoV-2, emphasizing the importance of accounting for disease-related changes in protein binding of imatinib. Conversely, the unbound concentration of imatinib was predicted to be far less sensitive to variation in plasma AAG concentrations, where an increase from typical values in healthy and cancer populations of 0.8 to 0.9 g/L to 1.8 g/L observed in patients with SARS-CoV-2 infection,[7,42] led to only around 30% changes in predicted unbound $C_{ss,max}$ and $C_{ss,min}$ of imatinib (Figure S1B). Hepatic CYP2C8 was predicted to be of more importance to systemic exposures of imatinib at steady state, for both total (Figure S1) and unbound concentrations of the drug (not shown), than hepatic CYP3A4. This was mainly due to autoinhibition of the latter following chronic administration of imatinib.[14] Nevertheless, the typical population value of CYP2C8 abundance was implemented throughout the PBPK simulations due to the lack of clinical and/or in vitro data to support the reduction of CYP2C8 activity in moderate to severe SARS-CoV-2 infection. Variation in protein level of CYP3A4 in enterocytes was predicted to have a negligible impact on plasma concentrations of imatinib, in line with high bioavailability of imatinib.[33]

A sensitivity analysis of abundances in hepatic P-gp and BCRP from 0.1- to 10-fold of the default values in healthy European populations suggested little to no effect on systemic exposure of imatinib. This trend may be explained by the limited role of P-gp– and BCRP-mediated biliary clearance of imatinib, which in total contributes to ≈30% to total imatinib clearance. The extent of interaction between imatinib and dexamethasone may substantially be affected by the concentration that provides half of the maximum fold induction of dexamethasone assigned to the model, particularly when the value was lowered by 2 or 3 orders of magnitude (Figure S1H). However, further verifications using a range of CYP3A substrates are warranted.

Lack of significant differences in unbound concentrations of imatinib between the CML/GIST cohort and the patient population with SARS-CoV-2 [7] was unsurprising, since imatinib has a low hepatic extraction ratio.[9] Hence, changes in the extent of protein binding of imatinib due to SARS-CoV-2 infection affected the total but not unbound drug clearance. This was also the case for lopinavir, which also extensively binds to plasma AAG, in patients with SARS-CoV-2 infection.[43] Therefore, unbound trough concentrations ($C_{ss,min,u}$) of imatinib are likely to be a clinically relevant exposure metric to predict treatment outcomes in patients with SARS-CoV-2 and CML/GIST. However, monitoring imatinib $C_{ss,min,u}$ may present logistical and analytical issues.[8] More importantly, the desirable range for imatinib $C_{ss,min,u}$ has not been as well established as that of $C_{ss,min}$.[44] It is also noteworthy that the dynamic of SARS-CoV-2–induced changes in plasma AAG level over time (ie, the time required for the elevated AAG to reach the baseline value after recovery from SARS-CoV-2 infection) is yet to be determined.

Acute and chronic hepatic and renal impairments were among the exclusion criteria for the patient cohort with SARS-CoV-2 from which the imatinib pharmacokinetic data was taken and, thus, no further adjustments in blood flows to liver and kidney tissue compartments in the PBPK simulations were necessary. However, this needs to be accounted for in the PBPK simulations of patients with severe SARS-CoV-2 infection.[4,6,45] While PBPK modeling strategies to simulate pharmacokinetic profiles in patients with chronic liver impairment (Child-Pugh A to C cirrhosis) has been established,[46,47] physiological changes in acute liver failure pertinent to drug pharmacokinetics are less clear and, hence, may pose a challenge in the implementation of PBPK modeling approaches in patients with SARS-CoV-2 with hepatic complications. Despite accumulating evidence of lower abundances of many CYP and non-CYP enzymes in chronic liver impairment,[48,49] the corresponding data from patients

Table 2. Potential Enablers and Barriers to Implementation of a PBPK Modeling Approach for Prediction of Drug Pharmacokinetics in Patients With SARS-CoV-2 Infection

Points to Consider	Enablers	Barriers
Development of a virtual SARS-CoV-2 patient population	A PBPK modeling approach enables a systematic and comprehensive integration of different physiological factors underpinning interpatient variability in drug pharmacokinetics. Several dedicated PBPK platforms have been developed with predefined validated PBPK equations and a constantly maintained database related to system parameters, ensuring reliability of the modeling and simulation workflow.[62,63]	There is a paucity of clinical data on (patho)physiological characteristics and protein level or in vivo activity of drug metabolizing enzymes and transporters in patients with SARS-CoV-2 infection. It is not always possible to discern the extent of changes in physiological parameters of interest in patients with severe SARS-CoV-2 infection from those of moderate or mild infection due to the nature of the clinical data. Effect of disease-related changes in fu_p and activity of drug transporters on volume of distribution has not been accounted for in the current PBPK platforms.[23,24]
A complex interplay between SARS-CoV-2 infection and comorbidities	Established knowledge and increasingly common use of a PBPK modeling approach to predict drug concentrations in disease and special patient populations, particularly patients with renal and hepatic (cirrhosis) impairments, obese population, and older adults[47,64–66]	There was a trend for overestimation of systemic drug exposures in patients with chronic kidney and liver failures, where the prediction fold-differences of PBPK models tended to be higher with increasing severity of the organ impairment[46] The extent of pathophysiological changes in chronic impairment of the eliminating organs may differ from those of acute organ impairment, the latter of which are more frequently associated with SARS-CoV-2 infection.[2,6]
PBPK model representation of suppression of CYP enzymes by proinflammatory mediators, particularly IL-6	PBPK modeling strategies to account for CYP3A suppression by IL-6 in general inflammatory diseases has been proposed,[67] which was recently extrapolated to SARS-CoV-2 infection.[68]	Dexamethasone has become one of the staple drugs for treatment of patients being hospitalized with SARS-CoV-2 infection. Dexamethasone is a weak to moderate CYP3A inducer that may as well downregulate the synthesis of IL-6 and, thus, attenuating the CYP3A suppression effect by the cytokine. A more complex model may be required to physiologically represent the dynamic interplay between dexamethasone and IL-6 in regulating in vivo CYP3A activity.
Further verifications of the PBPK models for SARS-CoV-2 patient population	Clinical pharmacokinetic data for new and repurposed drugs intended for treatment of SARS-CoV-2 infection or associated comorbidities is accumulating.	Most of the reported pharmacokinetic data in this patient population were derived from clinical studies with a sparse sampling strategy and oftentimes did not cover different spectrum of the disease severity. Comorbidities and potential for drug interactions in patient cohorts from which the pharmacokinetic data was extracted should be accounted for during verifications of the PBPK model.
Prediction of local drug concentrations in lung tissues	A permeability-limited lung model has been proposed to predict drug disposition in lung tissues and ELF following intrapulmonary delivery or other routes of drug administration.[69,70]	Lack of robust human data for several important physiological components of the lung model (eg, prediction of drug permeability across each segment of the respiratory tract and mucocilliary turnover in inflamed lung tissues due to SARS-CoV-2 infection) may limit the generalization of the model.

CYP, cytochrome P450; ELF, epithelial lining fluid; fu_p, unbound fraction in plasma; IL-6, interleukin-6; PBPK, physiologically based pharmacokinetic; SARS-CoV-2, severe acute respiratory syndrome coronavirus 2.

with acute liver failure is lacking. Interestingly, a dose-dependent decrease in mRNA level of CYP3A11, the murine ortholog of human CYP3A4 enzyme, was observed in a mouse model of acetaminophen-induced acute liver injury.[50] It is noteworthy that changes in abundance and/or activity of CYP enzymes related to acute liver injury, the suppression effect of proinflammatory cytokines and interactions with comedications may all contribute to the net in vivo phenotype of the enzymes in patients with SARS-CoV-2 infection. A

meta-analysis comparing in vitro activity and/or protein level of a range of CYP enzymes between healthy individuals and patients with cancer led to inconclusive results.[51] Proinflammatory mediators, particularly IL-6 that may suppress CYP3A activity, have been linked to disease progression in patients with advanced cancers.[52] However, systemic exposures to midazolam, a selective and sensitive CYP3A probe drug, in patients with advanced solid tumors (including GIST) were similar to that in healthy populations,[53] supporting

the notion that CYP3A activity is relatively unaltered in patients with cancer.[51] Hence, no modification was made on abundances of CYP3A4 and CYP2C8 enzymes throughout the PBPK simulations of imatinib in this study. It is interesting to note that imatinib has been reported to cause drug-induced liver injury, although this adverse effect is relatively rare and idiosyncratic in nature.[54]

Acute kidney injury (AKI) is one of the frequent complications or comorbidities of patients hospitalized with moderate to severe SARS-CoV-2 infection.[3,4] Cancer may also increase the likelihood of acute and chronic renal impairment. The underlying mechanisms are not entirely clear, but the risk of developing renal injuries appears to be higher in patients with urological cancers and those undergoing treatment with cytotoxic drugs that may induce nephrotoxicity.[55] Kidney dysfunction is also a relatively common presenting symptoms among patients with multiple myeloma, which can be reversed in most cases as the cancer being treated.[56] Interestingly, treatment with imatinib has been associated with a higher risk for chronic renal impairment. There was a downward trend of the estimated glomerular filtration rate in patients with CML over 4 years of treatment with imatinib before stabilizing.[57] As is the case with chronic kidney disease, AKI may lead to a substantial decrease in renal drug clearance and hepatic CYP2C8 activity, the latter of which is likely due to the accumulation of uremic toxins.[58,59] However, clinical data in patients with AKI to support this is currently limited. Renal impairment is unlikely to affect the systemic exposure to imatinib due to very low contribution of renal elimination to the overall drug clearance (Table S1). Nevertheless, potential changes in CYP2C8 activity and plasma protein concentrations should be accounted for in the PBPK simulations to simulate patients with SARS-CoV-2 infection and AKI. It is also worth noting that patients with cancers typically have lower plasma albumin concentrations compared to healthy populations, with a more extensive decrease in albumin concentrations as disease progresses.[51,53] Similarly, hypoalbuminemia has been associated with patients with severe SARS-CoV-2 infection or in critical care.[60,61] Nevertheless, the disease-related changes in plasma albumin concentrations are unlikely to affect imatinib pharmacokinetics as the drug has higher affinity toward plasma AAG compared to albumin.[8]

Other (patho)physiological changes observed in patients with SARS-CoV-2 infection, along with knowledge gaps and critical evaluations on potential barriers and enablers for successful implementation of PBPK modeling approaches in the patient population with SARS-CoV-2, are outlined in Figure 2 and Table 2. More comprehensive clinical data on (patho)physiological changes relevant for drug disposition stratified by disease severity, and further verification with larger clinical pharmacokinetic data, are warranted for generalization of the PBPK modeling approach in patients with SARS-CoV-2 infection.

Conclusion

In conclusion, a PBPK modeling approach was successfully implemented to predict imatinib pharmacokinetics in patients with SARS-CoV-2 infection, by accounting for disease-associated changes in plasma AAG concentration and the potential drug interaction between imatinib and dexamethasone. Despite this promising finding, a refinement of the virtual SARS-CoV-2 population model by comprehensively accounting for physiological characteristics of the patient population and further verification using different drugs used for treatment of SARS-CoV-2 infection or comorbidities are desirable.

Acknowledgment

Conflicts of Interest

The authors have no conflict of interest to declare.

Funding

Author Contributions

J.A. performed the simulations, analyzed the data, and drafted the manuscript; J.A.A., A.V.B., and A.J.M. contributed to the interpretation and critically revised the manuscript.

Data Availability Statement

Data available from the authors upon reasonable request.

References

1. Wiersinga WJ, Rhodes A, Cheng AC, Peacock SJ, Prescott HC. Pathophysiology, transmission, diagnosis, and treatment of coronavirus disease 2019 (COVID-19): a review. *JAMA*. 2020;324(8):782-793.

2. Legrand M, Bell S, Forni L, et al. Pathophysiology of COVID-19-associated acute kidney injury. *Nat Rev Nephrol*. 2021;17(11):751-764.

3. Fisher M, Neugarten J, Bellin E, et al. AKI in hospitalized patients with and without COVID-19: a comparison study. *J Am Soc Nephrol*. 2020;31(9):2145-2157.

4. Hirsch JS, Ng JH, Ross DW, et al. Acute kidney injury in patients hospitalized with COVID-19. *Kidney Int*. 2020;98(1):209-218.

5. Marjot T, Webb GJ, Barritt ASt, et al. COVID-19 and liver disease: mechanistic and clinical perspectives. *Nat Rev Gastroenterol Hepatol*. 2021;18(5):348-364.

6. Phipps MM, Barraza LH, LaSota ED, et al. Acute liver injury in COVID-19: prevalence and association with clinical outcomes in a large U.S. cohort. *Hepatology*. 2020;72(3):807-817.

7. Bartelink IH, Bet PM, Widmer N, et al. Elevated acute phase proteins affect pharmacokinetics in COVID-19 trials: lessons from the CounterCOVID - imatinib study. *CPT Pharmacometrics Syst Pharmacol*. 2021;10(12):1497-1511.

8. Haouala A, Widmer N, Guidi M, et al. Prediction of free imatinib concentrations based on total plasma concentrations in patients with gastrointestinal stromal tumours. *Br J Clin Pharmacol*. 2013;75(4):1007-1018.

9. Barratt DT, Somogyi AA. Role of pharmacogenetics in personalised imatinib dosing. *Trans Cancer Res*. 2017;6(Suppl 10):S1541-S1557.

10. Widmer N, Decosterd LA, Csajka C, et al. Population pharmacokinetics of imatinib and the role of alpha-acid glycoprotein. *Br J Clin Pharmacol*. 2006;62(1):97-112.

11. Adiwidjaja J, Boddy AV, McLachlan AJ. Implementation of a physiologically based pharmacokinetic modelling approach to guide optimal dosing regimens for imatinib and potential drug interactions in paediatrics. *Front Pharmacol*. 2020;10(1672):1-18.

12. Smith P, Bullock JM, Booker BM, Haas CE, Berenson CS, Jusko WJ. The influence of St. John's wort on the pharmacokinetics and protein binding of imatinib mesylate. *Pharmacotherapy*. 2004;24(11):1508-1514.

13. Filppula AM, Tornio A, Niemi M, Neuvonen PJ, Backman JT. Gemfibrozil impairs imatinib absorption and inhibits the CYP2C8-mediated formation of its main metabolite. *Clin Pharmacol Ther*. 2013;94(3):383-393.

14. Filppula AM, Neuvonen M, Laitila J, Neuvonen PJ, Backman JT. Autoinhibition of CYP3A4 leads to important role of CYP2C8 in imatinib metabolism: variability in CYP2C8 activity may alter plasma concentrations and response. *Drug Metab Dispos*. 2013;41(1):50-59.

15. Rowland-Yeo K, Jamei M, Yang J, Tucker GT, Rostami-Hodjegan A. Physiologically based mechanistic modelling to predict complex drug-drug interactions involving simultaneous competitive and time-dependent enzyme inhibition by parent compound and its metabolite in both liver and gut - the effect of diltiazem on the time-course of exposure to triazolam. *Eur J Pharm Sci*. 2010;39(5):298-309.

16. Adiwidjaja J, Gross AS, Boddy AV, McLachlan AJ. Physiologically-based pharmacokinetic model predictions of inter-ethnic differences in imatinib pharmacokinetics and dosing regimens. *Br J Clin Pharmacol*. 2022;88(4):1735-1750.

17. Aman J, Duijvelaar E, Botros L, et al. Imatinib in patients with severe COVID-19: a randomised, double-blind, placebo-controlled, clinical trial. *Lancet Respir Med*. 2021;9(9):957-968.

18. Recovery Collaborative Group, Horby P, Lim WS, et al. Dexamethasone in hospitalized patients with COVID-19. *N Engl J Med*. 2021;384(8):693-704.

19. Lutz JD, Mathias A, German P, Pikora C, Reddy S, Kirby BJ. Physiologically-based pharmacokinetic modeling of remdesivir and its metabolites to support dose selection for the treatment of pediatric patients with COVID-19. *Clin Pharmacol Ther*. 2021;109(4):1116-1124.

20. European Medicines Agency, Human Medicines Division. Summary on compassionate use: Remdesivir Gilead. Accessed April 29, 2022. https://www.ema.europa.eu/en/documents/other/summary-compassionate-use-remdesivir-gilead_en.pdf

21. Spoorenberg SM, Deneer VH, Grutters JC, et al. Pharmacokinetics of oral vs. intravenous dexamethasone in patients hospitalized with community-acquired pneumonia. *Br J Clin Pharmacol*. 2014;78(1):78-83.

22. Reckers A, Wu AHB, Ong CM, Gandhi M, Metcalfe J, Gerona R. A combined assay for quantifying remdesivir and its metabolite, along with dexamethasone, in serum. *J Antimicrob Chemother*. 2021;76(7):1865-1873.

23. Ye M, Nagar S, Korzekwa K. A physiologically based pharmacokinetic model to predict the pharmacokinetics of highly protein-bound drugs and the impact of errors in plasma protein binding. *Biopharm Drug Dispos*. 2016;37(3):123-141.

24. Benet LZ, Bowman CM, Liu S, Sodhi JK. The extended clearance concept following oral and intravenous dosing: theory and critical analyses. *Pharm Res*. 2018;35(12):242.

25. Widmer N, Decosterd LA, Leyvraz S, et al. Relationship of imatinib-free plasma levels and target genotype with efficacy and tolerability. *Br J Cancer*. 2008;98(10):1633-1640.

26. Widmer N, Decosterd LA, Csajka C, et al. Imatinib plasma levels: correlation with clinical benefit in GIST patients. *Br J Cancer*. 2010;102(7):1198-1199.

27. Delbaldo C, Chatelut E, Re M, et al. Pharmacokinetic-pharmacodynamic relationships of imatinib and its main metabolite in patients with advanced gastrointestinal stromal tumors. *Clin Cancer Res*. 2006;12(20):6073-6078.

28. Pursche S, Schleyer E, von Bonin M, et al. Influence of enzyme-inducing antiepileptic drugs on trough level of imatinib in glioblastoma patients. *Curr Clin Pharmacol*. 2008;3(3):198-203.

29. van Erp NP, Gelderblom H, Karlsson MO, et al. Influence of CYP3A4 inhibition on the steady-state pharmacokinetics of imatinib. *Clin Cancer Res*. 2007;13(24):7394-7400.

30. Jacobs TG, Marzolini C, Back DJ, Burger DM. Dexamethasone is a dose-dependent perpetrator of drug-drug interactions: implications for use in people living with HIV. *J Antimicrob Chemother*. 2022;77(3):568-573.

31. Honorat M, Mesnier A, Di Pietro A, et al. Dexamethasone down-regulates ABCG2 expression levels in breast cancer cells. *Biochem Biophys Res Commun*. 2008;375(3):308-314.

32. Pavek P, Merino G, Wagenaar E, et al. Human breast cancer resistance protein: interactions with steroid drugs, hormones, the dietary carcinogen 2-amino-1-methyl-6-phenylimidazo(4,5-b)pyridine, and transport of cimetidine. *J Pharmacol Exp Ther*. 2005;312(1):144-152.

33. Peng B, Dutreix C, Mehring G, et al. Absolute bioavailability of imatinib (Glivec) orally versus intravenous infusion. *J Clin Pharmacol*. 2004;44(2):158-162.

34. Tomlinson ES, Lewis DF, Maggs JL, Kroemer HK, Park BK, Back DJ. In vitro metabolism of dexamethasone (DEX) in human liver and kidney: the involvement of CYP3A4 and CYP17 (17,20 LYASE) and molecular modelling studies. *Biochem Pharmacol*. 1997;54(5):605-611.

35. Ke AB, Milad MA. Evaluation of maternal drug exposure following the administration of antenatal corticosteroids during late pregnancy using physiologically-based pharmacokinetic modeling. *Clin Pharmacol Ther*. 2019;106(1):164-173.

36. Aziz M, Fatima R, Assaly R. Elevated interleukin-6 and severe COVID-19: a meta-analysis. *J Med Virol*. 2020;92(11):2283-2285.

37. Said EA, Al-Reesi I, Al-Shizawi N, et al. Defining IL-6 levels in healthy individuals: a meta-analysis. *J Med Virol.* 2021;93(6):3915-3924.

38. Herold T, Jurinovic V, Arnreich C, et al. Elevated levels of IL-6 and CRP predict the need for mechanical ventilation in COVID-19. *J Allergy Clin Immunol.* 2020;146(1):128–136 e124.

39. Lenoir C, Terrier J, Gloor Y, et al. Impact of SARS-CoV-2 infection (COVID-19) on cytochromes P450 activity assessed by the Geneva cocktail. *Clin Pharmacol Ther.* 2021;110(5):1358-1367.

40. WHO Rapid Evidence Appraisal for COVID-19 Therapies Working Group, Shankar-Hari M, Vale CL, et al. Association between administration of IL-6 antagonists and mortality among patients hospitalized for COVID-19: a meta-analysis. *JAMA.* 2021;326(6):499-518.

41. National Institutes of Health. Coronavirus Disease 2019 (COVID-19) Treatment Guidelines. Accessed April 29, 2022. https://www.covid19treatmentguidelines.nih.gov

42. Bins S, Eechoute K, Kloth JS, et al. Prospective analysis in GIST patients on the role of alpha-1 acid glycoprotein in imatinib exposure. *Clin Pharmacokinet.* 2017;56(3):305–310.

43. Stanke-Labesque F, Concordet D, Djerada Z, et al. Neglecting plasma protein binding in COVID-19 patients leads to a wrong interpretation of lopinavir overexposure. *Clin Pharmacol Ther.* 2021;109(4):1030-1033.

44. Gotta V, Widmer N, Decosterd LA, et al. Clinical usefulness of therapeutic concentration monitoring for imatinib dosage individualization: results from a randomized controlled trial. *Cancer Chemother Pharmacol.* 2014;74(6):1307-1319.

45. Vitiello A, La Porta R, D'Aiuto V, Ferrara F. The risks of liver injury in COVID-19 patients and pharmacological management to reduce or prevent the damage induced. *Egypt Liver J.* 2021;11(1):1-6.

46. Heimbach T, Chen Y, Chen J, et al. Physiologically-based pharmacokinetic modeling in renal and hepatic impairment populations: a pharmaceutical industry perspective. *Clin Pharmacol Ther.* 2021;110(2):297-310.

47. Johnson TN, Boussery K, Rowland-Yeo K, Tucker GT, Rostami-Hodjegan A. A semi-mechanistic model to predict the effects of liver cirrhosis on drug clearance. *Clin Pharmacokinet.* 2010;49(3):189-206.

48. Prasad B, Bhatt DK, Johnson K, et al. Abundance of phase 1 and 2 drug-metabolizing enzymes in alcoholic and hepatitis C cirrhotic livers: a quantitative targeted proteomics study. *Drug Metab Dispos.* 2018;46(7):943-952.

49. El-Khateeb E, Al-Majdoub ZM, Rostami-Hodjegan A, Barber J, Achour B. Proteomic quantification of changes in abundance of drug-metabolizing enzymes and drug transporters in human liver cirrhosis: different methods, similar outcomes. *Drug Metab Dispos.* 2021;49(8):610-618.

50. Bao Y, Phan M, Zhu J, Ma X, Manautou JE, Zhong XB. Alterations of cytochrome P450-mediated drug metabolism during liver repair and regeneration after acetaminophen-induced liver injury in mice [published online ahead of print 2021]. *Drug Metab Dispos.* https://doi.org/10.1124/dmd.121.000459.

51. Mendes MS, Hatley O, Gill KL, Yeo KR, Ke AB. A physiologically based pharmacokinetic - pharmacodynamic modelling approach to predict incidence of neutropenia as a result of drug-drug interactions of paclitaxel in cancer patients. *Eur J Pharm Sci.* 2020;150:1-10.

52. Coutant DE, Kulanthaivel P, Turner PK, et al. Understanding disease-drug interactions in cancer patients: implications for dosing within the therapeutic window. *Clin Pharmacol Ther.* 2015;98(1):76-86.

53. Cheeti S, Budha NR, Rajan S, Dresser MJ, Jin JY. A physiologically based pharmacokinetic (PBPK) approach to evaluate pharmacokinetics in patients with cancer. *Biopharm Drug Dispos.* 2013;34(3):141-154.

54. Shah JM, Lin K, Etienne D, Reddy M, Liu Y. Imatinib-induced hepatitis in a patient treated for gastrointestinal stromal tumor: a rare adverse effect. *Cureus.* 2018;10(4):1-9.

55. Malyszko J, Tesarova P, Capasso G, Capasso A. The link between kidney disease and cancer: complications and treatment. *Lancet.* 2020;396(10246):277-287.

56. Faiman B, Doss D, Colson K, Mangan P, King T, Tariman JD. Renal, GI, and peripheral nerves: evidence-based recommendations for the management of symptoms and care for patients with multiple myeloma. *Clin J Oncol Nurs.* 2017;21(5 Suppl):19-36.

57. Yilmaz M, Lahoti A, O'Brien S, et al. Estimated glomerular filtration rate changes in patients with chronic myeloid leukemia treated with tyrosine kinase inhibitors. *Cancer.* 2015;121(21):3894-3904.

58. Tan ML, Yoshida K, Zhao P, et al. Effect of chronic kidney disease on nonrenal elimination pathways: a systematic assessment of CYP1A2, CYP2C8, CYP2C9, CYP2C19, and OATP. *Clin Pharmacol Ther.* 2018;103(5):854-867.

59. Lara-Prado JI, Pazos-Perez F, Mendez-Landa CE, et al. Acute kidney injury and organ dysfunction: what is the role of uremic toxins? *Toxins (Basel).* 2021;13(8):1-13.

60. Li J, Li M, Zheng S, et al. Plasma albumin levels predict risk for nonsurvivors in critically ill patients with COVID-19. *Biomark Med.* 2020;14(10):827-837.

61. Wu MA, Fossali T, Pandolfi L, et al. Hypoalbuminemia in COVID-19: assessing the hypothesis for underlying pulmonary capillary leakage. *J Intern Med.* 2021;289(6):861-872.

62. El-Khateeb E, Burkhill S, Murby S, Amirat H, Rostami-Hodjegan A, Ahmad A. Physiological-based pharmacokinetic modeling trends in pharmaceutical drug development over the last 20-years; in-depth analysis of applications, organizations, and platforms. *Biopharm Drug Dispos.* 2021;42(4):107-117.

63. Rostami-Hodjegan A, Bois FY. Opening a debate on open-source modeling tools: pouring fuel on fire versus extinguishing the flare of a healthy debate. *CPT Pharmacometrics Syst Pharmacol.* 2021;10(5):420-427.

64. Rowland Yeo K, Aarabi M, Jamei M, Rostami-Hodjegan A. Modeling and predicting drug pharmacokinetics in patients with renal impairment. *Expert Rev Clin Pharmacol.* 2011;4(2):261-274.

65. Ghobadi C, Johnson TN, Aarabi M, et al. Application of a systems approach to the bottom-up assessment of pharmacokinetics in obese patients: expected variations in clearance. *Clin Pharmacokinet.* 2011;50(12):809-822.

66. Chetty M, Johnson TN, Polak S, Salem F, Doki K, Rostami-Hodjegan A. Physiologically based pharmacokinetic modelling to guide drug delivery in older people. *Adv Drug Deliv Rev.* 2018;135(7):85-96.

67. Machavaram KK, Almond LM, Rostami-Hodjegan A, et al. A physiologically based pharmacokinetic modeling approach to predict disease-drug interactions: suppression of CYP3A by IL-6. *Clin Pharmacol Ther.* 2013;94(2):260-268.

68. Stader F, Battegay M, Sendi P, Marzolini C. Physiologically based pharmacokinetic modelling to investigate the impact of the cytokine storm on CYP3A drug pharmacokinetics in COVID-19 patients. *Clin Pharmacol Ther.* 2022;111(3):579-584.

69. Miller NA, Graves RH, Edwards CD, et al. Physiologically based pharmacokinetic modelling of inhaled nemiralisib: mechanistic components for pulmonary absorption, systemic distribution, and oral absorption. *Clin Pharmacokinet.* 2022;61(2):281-293.

70. Rowland Yeo K, Zhang M, Pan X, et al. Impact of disease on plasma and lung exposure of chloroquine, hydroxychloroquine and azithromycin: application of PBPK modeling. *Clin Pharmacol Ther*. 2020;108(5):976-984.

71. Herrmann J, Mori V, Bates JHT, Suki B. Modeling lung perfusion abnormalities to explain early COVID-19 hypoxemia. *Nat Commun*. 2020;11(1):1-9.

72. Ball L, Robba C, Herrmann J, et al. Lung distribution of gas and blood volume in critically ill COVID-19 patients: a quantitative dual-energy computed tomography study. *Crit Care*. 2021;25(1):1-12.

73. Caravita S, Baratto C, Di Marco F, et al. Haemodynamic characteristics of COVID-19 patients with acute respiratory distress syndrome requiring mechanical ventilation. An invasive assessment using right heart catheterization. *Eur J Heart Fail*. 2020;22(12):2228-2237.

74. Djakpo DK, Wang Z, Zhang R, Chen X, Chen P, Antoine M. Blood routine test in mild and common 2019 coronavirus (COVID-19) patients. *Biosci Rep*. 2020;40(8):1-5.

75. Huang J, Cheng A, Kumar R, et al. Hypoalbuminemia predicts the outcome of COVID-19 independent of age and comorbidity. *J Med Virol*. 2020;92(10):2152-2158.

76. Bajgain KT, Badal S, Bajgain BB, Santana MJ. Prevalence of comorbidities among individuals with COVID-19: a rapid review of current literature. *Am J Infect Control*. 2021;49(2):238-246.

77. Gasmi A, Peana M, Pivina L, et al. Interrelations between COVID-19 and other disorders. *Clin Immunol*. 2021;224:1-12.

Supplemental Information

Additional supplemental information can be found by clicking the Supplements link in the PDF toolbar or the Supplemental Information section at the end of web-based version of this article.